

Transcriptome Analysis Reveals Organ-Specific Effects of 2-Deoxyglucose Treatment in Healthy Mice

Ann E. Wells¹, John J. Wilson¹, Sarah E. Heuer^{1,2}, John D. Sears¹, Jian Wei¹, Raghav Pandey¹, Mauro W. Costa¹, Catherine C. Kaczorowski^{1,2,3}, Derry C. Roopenian¹, Chih-Hao Chang^{1,2,3*}, Gregory W. Carter^{1,2,3*}

¹The Jackson Laboratory, Bar Harbor, ME 04469, USA.

²Tufts University Graduate School of Biomedical Sciences, Boston, MA 02111, USA.

³Graduate School of Biomedical Sciences and Engineering, University of Maine, Orono, ME 04469, USA.

*Corresponding author

1 **Abstract**

2 **Objective:** Glycolytic inhibition via 2-deoxy-D-glucose (2DG) has potential therapeutic benefits
3 for a range of diseases, including cancer, epilepsy, systemic lupus erythematosus (SLE), and
4 rheumatoid arthritis (RA), and COVID-19, but the systemic effects of 2DG on gene function
5 across different tissues are unclear.

6 **Methods:** This study analyzed the transcriptional profiles of nine tissues from C57BL/6J mice
7 treated with 2DG to understand how it modulates pathways systemically. Principal component
8 analysis (PCA), weighted gene co-network analysis (WGCNA), analysis of variance, and
9 pathway analysis were all performed to identify modules altered by 2DG treatment.

10 **Results:** PCA revealed that samples clustered predominantly by tissue, suggesting that 2DG
11 affects each tissue uniquely. Unsupervised clustering and WGCNA revealed six distinct tissue-
12 specific modules significantly affected by 2DG, each with unique key pathways and genes. 2DG
13 predominantly affected mitochondrial metabolism in the heart, while in the small intestine, it
14 affected immunological pathways.

15 **Conclusions:** These findings suggest that 2DG has a systemic impact that varies across
16 organs, potentially affecting multiple pathways and functions. The study provides insights into
17 the potential therapeutic benefits of 2DG across different diseases and highlights the
18 importance of understanding its systemic effects for future research and clinical applications.

19

20 **Abbreviations**

21 2DG - 2-deoxy-D-glucose, RA - rheumatoid arthritis, SARS-CoV-2 - severe acute respiratory
22 syndrome coronavirus-2, SLE - systemic lupus erythematosus, ER - endoplasmic reticulum,
23 WGCNA - weighted gene co-network analysis, ANOVA - analysis of variance, PCA - Principal
24 component analysis, GSVA – Gene Set Variation Analysis, BCAA - branched-chain amino
25 acids, NAD⁺ - nicotinamide adenine dinucleotide

26 **Keywords:** 2-deoxy-D-glucose, C57BL/6J, metabolism, multi-tissue, transcriptomics

27 **1. Introduction**

28 2-deoxy-D-glucose (2DG) is a glucose analog that has garnered considerable interest in recent
29 years as a potential therapeutic agent for various diseases characterized by abnormal
30 glycolysis, including cancer[1-5], epilepsy[6], systemic lupus erythematosus (SLE)[7],
31 rheumatoid arthritis (RA)[8], and COVID-19 [9-12]. 2DG is taken up into cells by glucose
32 transporters and is converted by hexokinase into 2DG-6-phosphate which cannot be further
33 broken down to yield energy, resulting in a reduction in the rate of glycolysis[13]. Similarly, by
34 competing with mannose, 2DG disrupts the early steps of N-linked glycosylation, ultimately
35 resulting in the misfolding of proteins and the onset of endoplasmic reticulum (ER) stress[14].
36 Despite an increasing understanding of these cellular mechanisms, there remains a critical need
37 to delineate the specific mechanisms through which 2DG could be used to treat a range of
38 diseases and the organs that would be most affected in this context.

39
40 Studies have shown that 2DG can modulate progression or attenuation in multiple disease
41 paradigm. For instance, in anti-tumor effects, 2DG may act through energy restriction to prevent
42 tumor growth while maintaining bodyweight, glucose levels, and immunity[2, 4, 14, 15].
43 Furthermore, 2DG has been shown to reduce ATP due to its glycolytic properties and protein
44 synthesis through the AMPK/mTORC1 pathway, reducing translation and promoting
45 autophagy[16]. In seizure models, 2DG has been shown to reduce epileptic seizures both
46 acutely and chronically[6]. Additionally, in mice with traumatic brain injuries, cortical slices
47 showed reduced excitatory neurons and prevented epileptiform activity when treated
48 immediately with 2DG[6]. 2DG has also been shown to reduce amyloid precursor protein and
49 amyloid-beta oligomers in an Alzheimer's mouse model[17], delaying the progression of these
50 critical hallmarks of Alzheimer's disease. When treating autoimmune diseases, 2DG has
51 attenuated symptoms of SLE, RA, and multiple sclerosis in mice[7, 18]. Additionally, 2DG has
52 been shown to significantly extend the lifespan of SLE-prone mice compared to untreated

53 controls[7]. In these and several other examples, 2DG has shown early promise in both disease
54 prevention and attenuation.

55
56 The use of 2DG in cancer therapy has been limited and its therapeutic efficacy has been
57 inconsistent, but it has been shown to be well tolerated with no significant safety concerns
58 raised[5, 13]. Moreover, glycolytic inhibition has been shown to reduce viral replication[11, 19],
59 and 2DG is currently being investigated for its potential to treat severe acute respiratory
60 syndrome coronavirus-2 (SARS-CoV-2)[9-12]. In clinical trials, patients with moderate to severe
61 SARS-CoV-2 infection who were administered oral 2DG showed an improvement in their
62 symptoms and were taken off oxygen supplementation significantly earlier compared to patients
63 treated with standard of care therapies[12]. Although 2DG has shown the potential to ameliorate
64 multiple diseases, a better understanding of 2DG's systemic effects help to identify potential
65 targets for clinical trials in metabolic disorders.

66
67 Much of what is known concerning the effects of 2DG is based on studies of cell lines, selected
68 tissues, whole animal physiology, and disease. The current study, instead, sought to understand
69 the effects of 2DG administered systemically on major organs. Our goal was to understand how
70 2DG alters baseline metabolism of a genetically uniform population of young, healthy C57BL/6J
71 mice unencumbered by advanced age, disease, or manipulation. Our approach was to analyze
72 the transcriptomes of nine organs (heart, kidney, hippocampus, hypothalamus, prefrontal cortex,
73 skeletal muscle, small intestine, and spleen) from 2DG- and vehicle-treated C57BL/6J mice to
74 assess systemic responses to 2DG treatment (**Fig. 1**). Using a robust statistical filtering
75 strategy, which combined weighted gene co-network analysis (WGCNA), analysis of variance
76 (ANOVA), and correlation, our results show that 2DG altered metabolism, immunity, and
77 transcription in heart, small intestine, hypothalamus, prefrontal cortex, skeletal muscle, and liver
78 through a unique set of genes in each tissue. The small intestine presented an

79 immunomodulatory signature, while both heart and hypothalamus showed reduced
80 mitochondrial metabolism. Few pathways responded to 2DG in skeletal muscle and liver; and all
81 were down-regulated regardless of biological function. Pathways involved in RNA transcription
82 and endoplasmic reticulum (ER) stress in the prefrontal cortex were over and under-expressed
83 in response to 2DG, respectively. Our results provide a comprehensive understanding of the
84 systemic impact of 2DG on glycolysis and N-linked glycosylation and highlight the organ-specific
85 effects through which 2DG acts. Overall, our study lays the foundation for further research on
86 the therapeutic potential of targeting these metabolic pathways.

87

88 **2. Materials and Methods**

89 **2.1 Mice, Treatment, and Tissue Isolation**

90 C57BL/6J male mice (Jackson Laboratory, #000664), used in this study were bred and housed
91 at The Jackson Laboratory (Bar Harbor, Maine). Twenty mice at 8 and 20 mice at 11 weeks of
92 age were switched from a 6% (g/g) fat JL Mouse Breeder/Auto 6F (LabDiet[®] 5K52) diet to a
93 10% fat JL Mouse Breeder/Auto (LabDiet[®] 5K20) diet when moved into their mouse room,
94 provided with water *ad libitum*, and were housed on a 14-hour light, 10-hour dark cycle in a
95 specific pathogen-free room. 2-Deoxy-D-glucose (2DG, Thermo Fisher Scientific, category
96 number AC111980250, 99% purity) dissolved in drinking water at a concentration of 6 g/L was
97 provided to mice *ad libitum* for either 4-day or 28-day treatment times. As the average mouse
98 consumed ~ 3.5 ml of water per day, this equates to a dosage of 800 mg/kg/d. The rationale for
99 selecting this dosing regime is that it has proven to be therapeutically effective and safe in
100 treatment of autoimmune disease in several mouse models[18, 20]. After allometric scaling, this
101 dosage approximates an accepted human dosage of ~65mg/kg/d. The 4-day treatment cohort
102 was provided 2DG-water starting at 12 weeks of age, while the 28-day treatment cohort was
103 provided 2DG-water starting at 9 weeks of age (**Fig. 1**). Control mice received regular drinking
104 water with no additives. All mice, including age-matched control mice, were sacrificed at 13

105 weeks of age via cervical dislocation. Brains were removed and dissected to isolate the
106 hippocampus, hypothalamus, and pre-frontal cortex. Spleen, liver, heart, kidney, skeletal muscle
107 from left hind-leg and intestinal ileum were also harvested. Heart and intestine were flushed with
108 saline post-dissection to remove blood and feces, respectively. All harvested organs were
109 stored in RNAlater for subsequent RNA-seq analysis. The Jackson Laboratory Institutional
110 Animal Care and Use Committee (IACUC) approved all procedures.

111

112 **2.2 RNA Sequencing**

113 RNA-sequencing (RNA-seq) was performed by Omega Bioservices. Bulk RNA of the 9 excised
114 tissues (heart, hippocampus, hypothalamus, kidney, liver, prefrontal cortex, skeletal muscle,
115 small intestine, and spleen) (4 samples per treatment and time combination) was isolated with
116 the QIAGEN miRNeasy mini extraction kit (QIAGEN) and cDNA was synthesized with the High-
117 Capacity cDNA Reverse Transcription Kit (Applied Biosystems). RNA quality was assessed with
118 a Bioanalyzer 2100 (Agilent Technologies). Poly(A)-selected RNA-seq libraries were generated
119 using the Illumina TruSeq RNA Sample preparation kit v2. RNA-seq was performed in a 150-bp
120 paired-end format with a minimum of 40 million reads per sample on the Illumina HiSeq platform
121 according to the manufacturer's instructions. RNA-seq reads were filtered and trimmed for
122 quality scores >30 using a custom python script. The filtered reads were aligned to *Mus*
123 *musculus* GRCm38 using RSEM (v1.2.12) (58) with Bowtie2 (v2.2.0)[21] (command: rsem-
124 calculate-expression -p 12 --phred33-quals --seed-length 25 --forward-prob 0 --time --output-
125 genome-bam -- bowtie2). RSEM calculates expected counts and transcript per million (TPM).
126 The expected counts from RSEM were used in the Bioconductor edgeR 3.20.9 package[22-24]
127 to determine differentially expressed genes.

128

129 **2.3 Statistical Analysis**

130 All statistical analysis was performed in the language R (3.6.0/4.1.0)[25] equipped with RStudio.

131 The analytical strategy is summarized in Figure 1 and explained in subsequent method
132 sections.

133

134 **2.3.1 Principal Component Analysis**

135 Principal component analysis (PCA) was performed to identify whether samples clustered
136 based on treatment, time, or treatment-by-time interaction. The PCA algorithm was
137 implemented using the function `prcomp()` in the package `stats`[25]. Hotelling's T^2 ellipses were
138 used to identify the 95% confidence intervals for each cluster.

139

140 **2.3.2 Weight Gene Co-network Analysis**

141 To identify potential transcript networks Weighted Gene Co-Expression Network Analysis
142 (WGCNA) was performed using the `'WGCNA'` R package[26, 27]. Soft-thresholding power was
143 chosen so that the scale-free topology correlation hits as close to 0.9 as possible. The soft
144 thresholding powers chosen for heart, hippocampus, hypothalamus, kidney, liver, prefrontal
145 cortex, skeletal muscle, small intestine, and spleen were 5, 13, 9, 3, 3, 15, 13, and 20,
146 respectively. The adjacency matrix was created using `type = "unsigned"`. Dynamic tree cutting
147 was used to cluster metabolites and generate modules with a minimum of 15 genes in each
148 module. Networks were identified using all genes quantified by RNA-seq without replacement.
149 Module colors were assigned arbitrarily and have no bearing on functional annotation.

150

151 **2.3.3 Functional Pathway Analysis**

152 Overrepresentation pathway analysis was performed using `gProfiler2`[28]. KEGG and reactome
153 databases were used as the references to compare genes in each module identified in WGCNA
154 analysis, using `Ensembl 104` and `Ensembl Genomes 51` databases. To determine statistical
155 significance of each pathway identified, Fisher's exact test was used. P-values were adjusted
156 using the Benjamini-Hochberg procedure to reduce type 1 error ($FDR < 0.05$).

157

158 **2.3.4 Analysis of Variance using Aligned Rank Transformation**

159 Since the data was not normally distributed aligned rank transformation was performed using
160 the ARTool package[29, 30] to identify significance for using the linear model:

161

162
$$\text{Module eigengene} = \text{intercept} + \text{treat} + \text{time} + \text{treat}*\text{time}$$

163

164 to determine the effects of treatment, time, or treatment-by-time interaction on each module
165 eigengene.

166

167 Since the change in diet composition and time points overlap exactly, neither were individually
168 assessed in this study but they were evaluated in the ANOVA models—at the module, gene,
169 and Gene Set Variation Analysis (GSVA) level—for interaction to identify their combined
170 influence on treatment. Only modules, GSVA, and genes significant for treatment but not time or
171 treatment dependent on time were discussed.

172

173 **2.3.5 Mediation Analysis**

174 The R package mediation[31] was used to perform mediation analysis. Eigengenes for
175 overrepresented pathways were created using GSVA[32] (explained in section 2.6) and
176 assessed across tissues to determine if pathways were acting as mediators on the response to
177 treatment using two models; the mediator model:

178

179
$$\text{Pathway 1} = \text{intercept} + \text{treatment} + \text{time} + \text{treatment}*\text{time}$$

180

181 and the outcome model:

182
$$\text{Pathway 2} = \text{intercept} + \text{pathway 1} + \text{treatment} + \text{time} + \text{treatment}*\text{time}$$

183

184 The models were then entered into the function `mediate()` and simulated 1000 times.

185 Confidence intervals and p-values were created using the Quasi-Bayesian Monte Carlo method.

186

187 **2.4 Modules Identified Using Three Filtering Criteria**

188 To identify modules related to treatment for each tissue each module had to meet three criteria:

189 1.) module was significantly correlated with treatment, 2.) module identified significantly

190 overrepresented pathways, and 3.) module was uniquely significant for treatment only,

191 according to ANOVA. Correlation was used to directly describe the relationship between each

192 module and treatment. ANOVA was used to assess the difference between main effects and

193 their interactions. This filtering strategy was chosen to identify modules that had the most robust

194 response to 2DG treatment. Modules that fit these criteria were further assessed for genes that

195 may be central to the networks identified.

196

197 **2.5 Gene Set Variation Analysis**

198 GSEA was performed, using the GSEA package[32], to identify enrichment of significantly

199 overrepresented pathways for each tissue module (see data resource for comprehensive

200 description of all modules, section 2.6). To identify enriched pathways a reference set of

201 pathways is needed. To create the reference set of pathways, all ensembl genes listed for *Mus*

202 *musculus* were compared against the KEGG and reactome databases in gProfiler2 using the

203 `gost()` function and the ensembl 104 and ensembl genomes 51 databases. This identified 2,030

204 pathways, which were used as the pathway gene set. The set of genes in each module was

205 then assessed against the pathway gene set to identify significantly overrepresented pathways.

206 To calculate overrepresentation, we used the Fisher's exact test and corrected for multiple

207 comparisons using the Benjamini-Hochberg procedure ($FDR < 0.05$). To summarize the gene

208 expression in each pathway, the method `plage` was used, which uses the coefficients of the first

209 right-singular vector from the singular value decomposition. Genes within these overrepresented
210 pathways were then summarized into a singular eigengene representing their expression for
211 each sample. The pathway eigengenes for each significantly overrepresented pathway were
212 then tested using ANOVA:

213
$$\text{pathway eigengene} = \text{intercept} + \text{treat} + \text{time} + \text{treat} * \text{time}$$

214
215 to identify resident pathways significantly altered by treatment. This identified which significantly
216 overrepresented pathways were also significantly enriched.

217

218 **2.6 Data Resource Development for Reproducible and Transparent Data**

219 The data resource was developed using R 4.1.0, rmarkdown, and bookdown[33]. Static html
220 files were output using knitr and collated using a yaml file that controls the navigation bar on the
221 website and the general theme and layout, including footer information, and links in the
222 navigation bar to the shiny app, git repository, figshare, and contact information. The theme
223 used for the website was cerulean and type was set to inverse to change the color to dark blue.
224 The table of contents for each page was set to float. The website is publicly hosted at:
225 https://storage.googleapis.com/bl6_2dg_rnaseq/index.html.

226

227 **3. Results**

228 **3.1 Molecular changes are induced in a tissue-specific manner by 2-DG treatment**

229 The impact of 2DG on transcriptomic profiles of nine different tissues was assessed to identify
230 genes that were differentially expressed for treatment only. The number of differentially
231 expressed genes varied across the tissues, with a minimum of 230 genes in spleen and a
232 maximum of 1152 genes in hippocampus. Interestingly, only three tissues (muscle (1), small
233 intestine (119), and prefrontal cortex (3)) exhibited overrepresented pathways, indicating that
234 the effect of 2DG on biological pathways may be more significant in these tissues than in the

235 other six tissues examined. Assessing 2DG's effect at a granular level, however, do not account
236 for potential gene interactions. These findings suggest that assessing the correlation structure of
237 genes within each tissue may provide a better biological understanding of 2DG's impact at the
238 tissue level.

239
240 To identify the most robust signature in each tissue and minimize noise, a novel filtering strategy
241 was devised (**Fig. 1**). Principal Component Analysis showed that samples clustered by tissue
242 based on their transcriptomic profiles (**Fig. 2**). We used WGCNA to group genes into modules
243 that share highly correlated expression patterns. Across tissues, the number of modules into
244 which genes were clustered ranged from 25 to 46 and contained anywhere from 22 to 10,127
245 genes within each module. Identifying modules that fit the three criteria in the filtering strategy
246 (significant for treatment, through correlation and ANOVA, and contained significantly
247 overrepresented pathways ($p < 0.05$, $FDR < 0.05$)), we narrowed our focus to six tissues —
248 heart, hypothalamus, liver, skeletal muscle, prefrontal cortex, and small intestine — and
249 identified one module for each of these tissues. This approach allowed us to elucidate the most
250 robust changes in gene expression in response to 2DG treatment in each tissue and highlight
251 the biological pathways that are most affected. More information about the analysis, including
252 the number of modules and genes per tissue, can be found in the Supplementary Information or
253 on our website (https://storage.googleapis.com/bl6_2dg_rnaseq/index.html).

254

255

256 **3.2 2DG reduced expression of metabolic pathways in the heart**

257 The expression of genes in heart muscle was analyzed and found to cluster into 25 distinct
258 modules (**Supplementary Fig. 1A**), with three of them showing significant correlation with 2DG
259 treatment (**Supplementary Fig. 1B**). Further analysis using ANOVA revealed that only the
260 darkgreen module was uniquely significant for the treatment ($p < 0.001$). This module contained

261 138 genes predominantly related to metabolism (**Supplementary Fig. 1C**), which summary
262 eigengenes revealed were decreased in expression in 2DG-treated mice compared to control
263 mice (**Supplementary Fig. 1D, E**). The darkgreen module was found to contain ten pathways
264 related to mitochondrial metabolism and the breakdown of branched-chain amino acids (BCAA)
265 (**Table 1**), which were significantly overrepresented ($p < 0.05$). Comparison of genes within
266 each pathway using a Jaccard similarity index revealed that each pathway consisted of a unique
267 set of genes (**Supplementary Fig. 2**). To assess pathway enrichment, gene set variation
268 analysis (GSVA) was performed. Of the ten significantly overrepresented pathways, seven
269 showed significant reduction in eigengene expression for the treatment group only ($p < 0.05$,
270 **Supplementary Table 1**), referred to as high confidence pathways from this point forward.
271 BCAA degradation was found to be inversely correlated with changes in mitochondrial
272 metabolism, consistent with previous findings of mitochondrial dysfunction leading to BCAA
273 accumulation[34]. Failure in both mitochondrial metabolism and BCAA degradation have been
274 linked to increase cardiovascular disease[35], and reduced BCAA degradation has been
275 identified as a signature in heart failure[36]. The inverse relationship of BCAA degradation and
276 mitochondrial metabolism identified in this study suggests that 2DG's differential effects on heart
277 metabolism may provide protection against heart failure.

278

279 **Table 1: Metabolic pathways are overrepresented in the darkgreen heart module**

Pathways	GSVA Significance for Treatment (ANOVA p-value)*	GSVA Expression Direction (2DG compared to Control)
Metabolism	0.0001	Down
Mitochondrial translation	0.133	Down
Mitochondrial translation elongation	0.133	Down
Mitochondrial translation termination	0.133	Down
Propanoate metabolism	0.033	Down

Pyruvate metabolism	0.033	Down
Pyruvate metabolism and Citric Acid (TCA) cycle	0.004	Down
Regulation of pyruvate dehydrogenase (PDH) complex	0.001	Down
The citric acid (TCA) cycle and respiratory electron transport	0.001	Down
Valine, leucine, and isoleucine degradation	0.002	Up

280 * Significant p-values in bold

281

282 **3.3 2DG suppressed expression of immunological pathways in the small intestine**

283 The genes expressed in the small intestine were clustered into 46 modules (**Fig. 3A**). Three of
284 these modules were found to be significantly correlated for treatment ($p < 0.05$) and identified
285 significantly overrepresented pathways ($p < 0.05$), with the green4 module being uniquely
286 significant for treatment, according to ANOVA ($p = 0.04$, **Fig. 3B**). This module contained 467
287 genes (**Fig. 3E**) predominantly related to the immune system and summary eigengenes
288 revealed decreased expression in mice treated with 2DG compared to control mice (**Fig. 3C, D**).
289 Overrepresentation analysis identified 69 significant pathways ($p < 0.05$, **Supplementary Table**
290 **2**), containing a unique set of genes in each pathway according to the Jaccard similarity index
291 (**Supplementary Fig. 3**). GSEA results showed that 61 out of the 69 pathways were
292 significantly enriched for treatment only ($p < 0.05$, **Supplementary Table 2**) and therefore
293 indicated high confidence. Furthermore, when pathways were functionally annotated it was
294 noted that 39 of the 61 high confidence pathways were related to immunological function and
295 immunology related diseases. Thirteen pathways showed decreased gene expression in mice
296 treated with 2DG, while 26 pathways showed increased expression. The up-regulated pathways
297 were primarily involved in innate immunity and the down-regulated pathways were related to
298 adaptive immunity (**Supplementary Table 2**). CIBERSORT analysis was used to assess
299 immune cell types in the green4 module and found that nine cell types were determined to be

300 significantly different between the green4 module and all the genes identified within the small
301 intestine (referred to as all genes). Four of these cell types (eosinophils, macrophages, memory
302 B cells, and Th1 cells) were significantly increased in the green4 module compared to all genes
303 ($P < 0.05$). The expression of genes related to eosinophils and macrophages (innate immune
304 cells) increased with 2DG treatment, while genes related to memory B cells and Th1 cells
305 (adaptive immune cells) decreased, but not significantly. The expression of genes related to
306 immature dendritic cells was significantly different between the green4 module and all genes but
307 in a treatment-dependent manner, with decreased expression in the green4 module and mice
308 treated with 2DG compared to all genes and control mice (**Supplementary Table 3**).
309 Collectively, these results indicate that treatment with 2DG leads to changes in the gene
310 expression profile of the small intestine's immune system characterized by a reduction in
311 adaptive immunity, and potentially compensation for corresponding by an enrichment in innate
312 immune cells.

313

314 **3.4 2DG reduced expression of nicotinate metabolism in the liver**

315 A total of thirty-one modules were identified in liver (**Supplementary Fig. 4A**), but only the
316 darkolivegreen module, consisting of 280 genes that represented diverse functions met all three
317 filtering criteria (**Supplementary Fig. 4B, C**). The summary eigengenes revealed increased
318 expression in 2DG-treated mice compared to the control mice (**Supplementary Fig. 4D, E**). The
319 only significant pathway found was nicotinate metabolism, which was deemed to be of high
320 confidence through GSVA analysis. This pathway was overrepresented ($p < 0.05$,
321 **Supplementary Table 4**) and was significantly reduced in mice treated with 2DG compared to
322 the control group ($p = 0.008$). Nicotinate metabolism is important for maintaining levels of
323 nicotinamide adenine dinucleotide (NAD⁺), an important coenzyme necessary for energy
324 metabolism[37], which is primarily produced in the liver[38]. These findings suggest that 2DG
325 treatment may have an impact on NAD⁺ levels in the liver and thus on ATP production.

326

327 **3.5 2DG reduced expression of protein metabolism in skeletal muscle**

328 A comprehensive analysis of the skeletal muscle revealed the existence of 40 modules
329 (**Supplementary Fig. 5A**), of which 32 were found to have significantly overrepresented
330 pathways and three were significantly correlated with the treatment ($p < 0.05$, **Supplementary**
331 **Fig. 5B**). Further analysis revealed that among these three modules, only the salmon2 module
332 was determined to be unique and significant for treatment through ANOVA analysis ($p = 0.017$).
333 This module contained 153 genes (**Supplementary Fig. 5C**) and showed an increase in
334 summary eigengenes in mice treated with 2DG compared to the control mice (**Supplementary**
335 **Fig. 5D, E**). Like the findings in liver, genes in this module were found to be associated with a
336 myriad of functions, but only five pathways related to protein metabolism were significantly
337 overrepresented ($p < 0.05$, **Supplementary Table 5**) and showed a reduction in expression
338 after 2DG treatment. Further analysis using the Jaccard similarity index and GSVA revealed that
339 the genes involved in each pathway were unique (**Supplementary Fig. 6**), and two of the five
340 pathways were deemed uniquely significant for treatment and therefore high confidence ($p <$
341 0.05). As N-linked glycosylation is crucial for protein metabolism[39], the reduction in expression
342 may lead to up-regulation of the unfolded protein response and down-regulation of protein
343 synthesis. Overall, these data suggest that the treatment with 2DG has a significant impact on
344 the expression of genes related to protein metabolism in the skeletal muscle.

345

346 **3.6 2DG increased expression of fatty acid oxidation in the hypothalamus**

347 The genes expressed in the hypothalamus grouped into 25 modules (**Supplementary Fig. 7A**).
348 Four of these modules were found to be correlated with treatment (**Supplementary Fig. 7B**);
349 however, only the bisque4 module was uniquely significant for treatment ($p = 0.008$). This
350 module contained 289 genes predominantly related to metabolism and cell cycle
351 (**Supplementary Fig. 7C**). The summary eigengenes of this module were decreased in mice

352 treated with 2DG compared to the control mice (**Supplementary Fig. 7D, E**). Nine pathways
353 were significantly overrepresented ($p < 0.05$), and the Jaccard similarity index showed that the
354 genes identified in each pathway were unique (**Supplementary Fig. 8**). Functional annotation
355 revealed that these nine pathways were related to fatty acid oxidation and chromosome health.
356 Two of the overrepresented pathways (mitochondrial fatty acid beta-oxidation and mitochondrial
357 fatty acid beta-oxidation of saturated fatty acids) were uniquely enriched for treatment based on
358 GSVA analysis, supporting their high confidence ($p < 0.05$, **Supplementary Table 6**). Both
359 pathways were related to fatty acid oxidation, which often increases as a result of reduced
360 glycolysis[40]. Although the other seven pathways were not significantly enriched using GSVA,
361 the eigengenes in the G2/M DNA damage checkpoint pathway were negatively correlated with
362 each of the other eight pathways (**Supplementary Table 6**). The G2/M DNA checkpoint showed
363 significantly reduced expression in mice treated with 2DG ($p = 0.02$), but also for time ($p =$
364 0.036 , **Supplementary Table 6**). These results indicate that the hypothalamus increase fatty
365 acid oxidation in response to the blockade of glycolysis and protects DNA through upregulation
366 of pathways related to chromosome maintenance, potentially in response to the increase in
367 unfolded protein response[41]. Overall, these findings suggests that the hypothalamus may use
368 lipids as an alternative fuel source in response to 2DG.

369

370 **3.7 Enhancement of RNA transcription pathways by 2DG in the prefrontal cortex**

371 Thirty-six gene modules were identified in the prefrontal cortex (**Supplementary Fig. 9A**). Of
372 these, five modules showed a correlation with treatment ($p < 0.05$, **Supplementary Fig. 9B**)
373 and 26 modules contained significantly overrepresented pathways ($p < 0.05$), with only the
374 bisque2 module being uniquely significant for treatment, according to ANOVA ($p = 0.014$). The
375 bisque2 module consisted of 718 genes that represented many biological functions
376 (**Supplementary Fig. 9C**). The summary eigengenes were found to be elevated in 2DG-treated
377 mice compared to control mice (**Supplementary Fig. 9D, E**). Functional analysis revealed that

378 14 pathways were overrepresented in the bisque2 module ($p < 0.05$), with seven related to RNA
379 transcription and seven to protein metabolism. According to the Jaccard similarity index, the
380 genes in each pathway were found to be unique (**Supplementary Fig. 10**). Among these
381 pathways, 12 were considered high confidence pathways, as they showed significant
382 enrichment for treatment using GSEA ($p < 0.05$, **Supplementary Table 7**). 2DG increased the
383 overall expression of five high confidence pathways related to RNA transcription compared to
384 control mice. Conversely, the seven high confidence pathways related to protein metabolism
385 showed decreased expression in 2DG-treated mice compared to control mice. Although 2DG
386 decreased expression of the nucleotide excision repair pathways, it was negatively correlated
387 with other pathways that also showed decreased expression in response to 2DG. All pathways
388 related to RNA transcription were negatively correlated with pathways involved in protein
389 metabolism. These results indicate that in the prefrontal cortex protein metabolism and RNA
390 transcription both respond to 2DG. Their differential response to 2DG may protect the prefrontal
391 cortex from the accumulation of unfolded proteins caused by the disruption of N-linked
392 glycosylation.

393

394 **3.8 Tissue-specific responses to 2DG treatment revealed through correlation analysis of** 395 **gene modules**

396 Tissues act synergistically to maintain the health of the body, but each tissue expresses genes
397 at varying levels. In this study, the expression of the same genes was analyzed across tissues;
398 however, the comparison of the genes contained in each selected tissue module revealed
399 minimal gene overlap (**Fig. 4**). The highest number of genes shared across tissue modules,
400 although not significant ($p = 0.117$), was 18 between skeletal muscle and prefrontal cortex,
401 while the number of genes identified in each module ranged from 113 to 659. No gene was
402 shared by all tissues. Moreover, we also compared overrepresented pathways across tissues
403 and identified only one shared pathway between small intestine and prefrontal cortex

404 **(Supplementary Fig. 11)**. These results indicate that the tissue-specific effects of 2DG are
405 generally unique at both the gene and pathway levels.

406

407 We also identified distinct, organ-specific responses to 2DG that can be interpreted as a
408 network of co-occurring transcriptional changes across the organism (**Fig. 5**). To investigate the
409 relationships between tissue modules, we performed correlation analysis, resulting in five
410 significant pairwise relationships out of 21 ($p < 0.05$, **Fig. 5**). To gain a deeper understanding of
411 these relationships, we used GSVA eigengenes to examine the relationship of each pathway
412 across each tissue module. Positive correlations were found between small intestine and heart
413 tissues ($r = .51$, $p = 0.08$). Further assessment at the pathway level revealed a complex
414 relationship between adaptive and innate immunity in the small intestine and BCAA degradation
415 in the heart (**Fig. 5, Supplementary Table 8**). The pathways predominantly related to adaptive
416 immunity were inversely correlated with BCAA degradation, while those predominantly related
417 to innate immunity were positively correlated. Although lymphocytes do not remain in the heart
418 for any length of time, BCAA are necessary for lymphocyte development and clonal
419 expansion[42-45]. To assess any causal relationship between BCAA degradation and pathways
420 in the small intestine we performed causal mediation analysis. BCAA degradation did not
421 mediate any pathway's response to 2DG in the small intestine. These results indicate that while
422 there is an association between adaptive and innate immunity in the small intestine and BCAA
423 degradation in heart there is not causing the response to 2DG in the small intestine.

424

425 Tissue modules of the prefrontal cortex and hypothalamus were inversely related ($r = -0.48$, $p =$
426 0.09 , **Fig. 6**). The incorporation of 2DG into the oligosaccharide chain inhibits N-linked
427 glycosylation and can lead to the formation of unfolded glycoproteins and induce ER stress[19].
428 In response to ER stress, the cell cycle is arrested at the G2/M DNA damage checkpoint[46].
429 Our findings showed a positive correlation between the G2/M DNA checkpoint pathway in the

430 hypothalamus and pathways related to ER stress in the prefrontal cortex (**Fig. 7,**
431 **Supplementary Table 9**). To assess the potential causal relationship between the
432 hypothalamus and prefrontal cortex, we conducted a causal mediation analysis and observed
433 that the G2/M DNA damage checkpoint pathway had a direct effect across all pathways in the
434 prefrontal cortex ($p < 0.05$) but no causal mediated effects. This indicates that the activation of
435 the G2/M DNA damage checkpoint pathway may have been a secondary response to the ER
436 stress induced by 2DG treatment, rather than the primary cause of the differential response to
437 2DG. Overall, these results suggest that both the hypothalamus and prefrontal cortex respond
438 to the disruption of N-linked glycosylation by modulating the expression of pathways to
439 counteract ER stress and the accumulation of unfolded proteins.

440

441 **3.9 Data Resource**

442 While we highlighted results from six tissues that stood out based on our filtering strategy, the
443 data resource that accompanies this paper contains WGCNA and other analyses for each of the
444 nine tissues, all the tissues combined, the brain tissues combined, and spleen, skeletal muscle,
445 and small intestine combined. Additionally, analyses of all modules are present for the
446 investigation of genes and networks not discussed in this paper. To ensure transparency and
447 reproducibility a data resource was created to contain the analyses performed along with code,
448 plots, and analysis description. The data resource can be intuitively navigated to meet the
449 specific needs of individual researchers and is accessible through the link to the website
450 (https://storage.googleapis.com/bl6_2dg_rnaseq/index.html).

451

452 The website is organized in a user-friendly manner with each WGCNA analysis housed under
453 its own tab, classified by tissue or tissue combination. In addition to the WGCNA analysis, the
454 website includes pages dedicated to the distribution analysis, outlier assessment, and sample
455 information, as well as additional analyses performed for the paper. Researchers can access

456 the raw code repository via a link to figshare containing the entire project with data, including the
457 Shiny app, and a Shiny app for basic plots for any gene identified in this study.

458

459 **4. Discussion**

460 The systemic effects of 2DG across the body have applications for understanding the potential
461 downstream effects of 2DG therapy, which has shown promise in treating cancer, epilepsy,
462 polycystic kidney disease, autoimmune disease, and in delaying Alzheimer's disease onset[1, 2,
463 4, 6, 7, 17, 47-50], and is currently being used to treat SARS-CoV-2[9, 11, 12]. Although 2DG
464 therapy has shown promise in treating these conditions, there is lingering concerns
465 regarding its safety. To better understand the potential risks associated with this
466 treatment, our study investigated the systemic effects of 2DG on the transcriptomes of nine
467 tissues in healthy young mice. By developing a novel filtering strategy of multiple statistical tests
468 to identify robust genes and pathways affected by 2DG in multiple tissues, we found that
469 WGCNA identified between 25 and 46 modules for each tissue, but only assessing modules
470 with overrepresented pathways reduced the number of modules of interest for each tissue to
471 between 12 and 32. Modules correlated with treatment further reduced the number of modules
472 of interest to between zero and three for each tissue. Finally, ANOVA revealed that heart,
473 hypothalamus, prefrontal cortex, small intestine, skeletal muscle, and liver were significantly
474 associated with treatment and fit our filtering strategy. These six tissues were assessed for their
475 robust 2DG effects, independently and collectively. Kidney, hippocampus, and spleen did not
476 meet all the filtering criteria and therefore were not discussed (see data resource for their
477 analysis).

478

479 2DG uniquely altered pathways and genes within each tissue module; however, tissue
480 alterations could still be broadly identified as a result of glycolysis or N-linked glycosylation

481 disruption. Glycolysis is necessary for energy production while N-linked glycosylation is
482 necessary for protein function[39]. By analyzing the functions of our high confidence pathways,
483 four tissues appeared to be affected by inhibition of glycolysis: heart, small intestine,
484 hypothalamus, and liver. In contrast, we inferred that the remaining two tissues were affected by
485 disruption of N-linked glycosylation: the prefrontal cortex and skeletal muscle.

486

487 Our study showed that 2DG treatment reduced the expression of gene pathways related to ATP
488 production and glycolysis in the heart, both of which have been shown to play a role in heart
489 failure[35, 51, 52]. Our results are consistent with a previous study[9], demonstrating that 2DG
490 altered these pathways, but did not report any cardiac toxicity or significant changes in
491 pathways related to ER stress. Although we did not perform EKGs, we observe no signs of
492 heart trouble in the treated mice; moreover, patients with moderate to severe SARS-CoV-2 or
493 advanced tumors treated with 2DG in clinical trials also showed no significant adverse heart-
494 related effects due to this treatment[5, 10, 53]. Our findings suggest that there may be a strong
495 association between ATP production and glycolysis pathways and the incidence of heart failure.
496 Therefore, the reduction of these pathways by 2DG treatment may provide a new avenue for
497 developing therapies to target these metabolic processes and prevent or treat heart failure.
498 While 2DG inhibits glycolysis, leading to a decrease in ATP production, it may also stimulate
499 compensatory mechanisms that enhance oxidative phosphorylation, another pathway for ATP
500 production[3, 9]. These findings suggest that 2DG primarily modifies metabolism in the heart
501 and may have implications for developing new therapies for cardiovascular diseases, including
502 using 2DG to improve heart health.

503

504 The small intestine is a unique immunological tissue because as it is the site in which immune
505 cells, both sessile and recirculating, are continuously exposed to gut microfloral stimuli[54]. This

506 encounter results in intestinal lymphocytes and leukocytes in an activated state that is not found
507 in other organs of healthy mice. In agreement, we found that the small intestine was the only
508 tissue in which untreated mice showed a very strong immune signature. Treatment with 2DG, in
509 the small intestine resulted in a striking dampening of pathways associated with adaptive
510 immunity and enrichment of innate immune pathways. Our analysis using CIBERSORT
511 suggested that genes related to memory B cells and Th1 cells had decreased expression in
512 mice treated with 2DG, which is in line with other studies showing a reduction in B and T cells
513 and an increase in macrophages and eosinophils in the presence of 2DG[15, 55]. The increase
514 in gene expression related to innate immunity pathways in the small intestine suggests that 2DG
515 treatment may enhance the intestinal immune response against invading pathogens, while the
516 decrease in gene expression related to adaptive immunity pathways may weaken the immune
517 response against certain pathogens, potentially leading to increased susceptibility to infections.
518 Additionally, our findings have implications for the potential relationship between the immune
519 system and microbiome of the small intestine as the reduction in expression of memory B cell
520 genes in mice treated with 2DG may promote dysbiosis. We envision two possibilities to explain
521 the effects of 2DG on intestinal immune signature: 1) 2DG acts directly to eliminate on
522 activated adaptive lymphocytes or their antigen presenting cells; and 2), 2DG eliminates gut
523 bacteria that are the cause of immune stimulation. Our results emphasize the modulatory
524 effects of 2DG on immunity in the small intestine, which may have implications for the
525 development of new therapies for immune-related disorders.

526
527 Fatty acid oxidation is a critical process that helps to maintain energy homeostasis by providing
528 energy substrates for ATP production[56]. The increase in fatty acid oxidation pathways in the
529 hypothalamus with 2DG treatment may play a crucial role in the regulation of energy balance
530 and metabolism when glycolysis is limited[57]. Our findings suggest that an increase in fatty
531 acid oxidation pathways in the hypothalamus with 2DG may have positive implications for the

532 overall health of the mice and inform new therapeutic approaches for metabolic disorders, such
533 as obesity and diabetes, which are characterized by metabolic dysregulation[57]. This
534 therapeutic approach may result in a shift towards energy expenditure and may help to
535 counteract the effects of a high-fat diet or other metabolic disorders. However, further studies
536 are needed to investigate the long-term effects of 2DG treatment on metabolic disorders in
537 humans. Additionally, it is reported that treatment with 2DG in the 3xTgAD mouse model of
538 Alzheimer's disease increased expression of genes involved in ketone formation in the brain,
539 reduced pathology, and resulted in increased serum ketone bodies[17]. Our study has shown
540 that the hypothalamus switched to fatty acid oxidation in the presence of 2DG, suggesting a
541 propensity of this critical anatomical structure to compensate for a reduction in glycolysis by
542 utilizing fatty acids. Future studies could explore the potential benefits and limitations of
543 targeting fatty acid oxidation pathways in the hypothalamus for the treatment of metabolic and
544 neurodegenerative disorders.

545
546 Treatment with 2DG alters genes involved in protein metabolism in both the prefrontal cortex
547 and skeletal muscle, suggesting potential implications for various diseases. In the prefrontal
548 cortex, 2DG reduces gene expression in protein metabolism pathways in the ER compared to
549 controls, which is associated with brain function regulation[58]. Previous studies have shown
550 that by shutting down protein synthesis, 2DG can induce the unfolded protein response,
551 reducing ER stress[14]. This is of particular interest as the prefrontal cortex is susceptible to
552 dysregulation due to ER stress[59, 60], which is linked to neurological disorders such as
553 Alzheimer's and Parkinson's disease[61]. Further investigations into the potential applications of
554 altered protein metabolism pathways in the prefrontal cortex with 2DG treatment could be
555 crucial for developing effective therapies for neurological disorders. Similarly, in skeletal muscle,
556 prolonged ERK activation events were reduced in mice treated with 2DG compared to controls,
557 which may have implications for metabolic health. Although ERK1/2 activation is necessary for

558 maintenance of myofibers and neuromuscular synapses, prolonged activation can lead to
559 muscle weakness[62-64]. Moreover, ERK pathway overactivation in skeletal muscle can lead to
560 inflammation through activation of TNF- α , IL-6, IL-1 β , and contribute to metabolic disorders
561 such as type 2 diabetes and obesity[65, 66]. This agrees with another study, which reported that
562 2DG decreases ERK pathways, resulting in decreased inflammatory markers[65]. Targeting
563 ERK activation with 2DG in humans may have significant implications for the prevention and
564 treatment of various diseases. Furthermore, the reduction of prolonged ERK activation events in
565 the muscle and protein synthesis in the prefrontal cortex of mice treated with 2DG may also
566 reduce inflammation and protect against misfolded proteins, which could be important for
567 developing therapies for related diseases.

568

569 Our comparison between tissues showed that each tissue module was unique at the gene and
570 pathway level demonstrating that 2DG affected each tissue in a unique manner. Although
571 tissues responded uniquely, we did note potential relationships across tissues in response to
572 2DG. These findings demonstrate that the complex effects of 2DG on different tissues and
573 pathways in mice, suggesting that further research is needed to understand the implications of
574 these effects for overall health. However, our results also suggest that 2DG therapy has
575 promising potential for the treatment of a range of diseases that affect different tissues and
576 pathways in humans.

577

578 Although the present analysis sheds light on the effects of 2DG in male mice, there are several
579 avenues for further investigation to expand our understanding of its potential benefits. First, it
580 would be informative to explore whether female mice respond differently to 2DG. Second, due
581 to the change in diet composition the effects of dosage length could not be assessed
582 systemically. Third, while our filtering strategy identified robust tissues and module responses to
583 2DG, it is possible that other effects were not captured. Additionally, future research in disease

584 models and in human patients is needed to fully understand the potential implications for clinical
585 applications, and it should be noted that our study did not directly evaluate the safety of 2DG.
586 Nonetheless, our findings improve our understanding of 2DG's effects on healthy tissues, which
587 may have implications for its safety in the long term.

588

589 **5. Conclusion**

590 Given the increasing interest in therapeutic use of 2DG, the goal of this study was to provide a
591 systematic analysis of the transcriptomic consequences of glycolysis blockade by 2DG in major
592 organs and tissues of healthy mammals. As we found surprisingly little transcriptional overlap
593 among tissue types affected by 2DG treatment, the results are best explained by 2DG uniquely
594 affecting each tissue type. The results are most consistent with two mechanisms through which
595 2DG is considered to act: inhibition of glycolysis and of N-linked glycosylation. This study
596 provides a comprehensive resource on the effects of 2DG, a glycolytic inhibitor, on various
597 tissues in non-diseased C57BL/6J mice, including a complete dataset, code, plots, and analysis
598 descriptions for transparency and reproducibility. The website
599 (https://storage.googleapis.com/bl6_2dg_rnaseq/index.html) is user-friendly, enabling easy
600 navigation through all available analyses from all nine tissues. This system-wide
601 characterization of 2DG activity across multiple tissues has the potential to inform its targeted
602 therapeutic use, taking into account the mechanism relevant to each disease-affected tissue.
603 However, further studies are needed to fully understand the mechanisms underlying the
604 responses and determine their physiological significance.

605 **Funding:** This work was supported by NIH grant GM115518 to GWC., The Jackson Laboratory
606 Director's Innovation Fund (JAX-DIF 19000-18-19) and the Longevity Impetus Grant from Norn
607 Group to C-HC.

608

609 **CRedit authorship contribution statement**

AEW: Methodology, Writing-Original draft preparation, Software, Visualization, Formal analysis, Data Curation; **JJW:** Conceptualization, Methodology, Writing-Review and Editing, Project administration; **SEH:** Investigation, Writing-Review and Editing; **JDS:** Investigation; **JW:** Investigation; **RP:** Conceptualization; **MWC:** Conceptualization, Writing-Review and Editing; **CCK:** Conceptualization, Methodology, Supervision, Resources, Funding acquisition; **DCR:** Conceptualization, Methodology, Resources, Writing-Review and Editing; **C-HC:** Conceptualization, Methodology, Supervision, Resources, Writing-Review and Editing, Project administration, Funding acquisition; **GWC:** Supervision, Resources, Writing-Review and Editing, Funding acquisition.

610

611 **Declaration of Competing Interest**

612 The authors declare no conflict of interest.

613

614 **Acknowledgements**

615 We would like to thank Selcan Aydin for her invaluable discussions regarding the statistical
616 approach and in proofreading the data resource. We thank Tamar Abel for proofreading the
617 data resource. We thank Grace Stafford for aligning the transcriptomes and providing the
618 processed RNA-seq data.

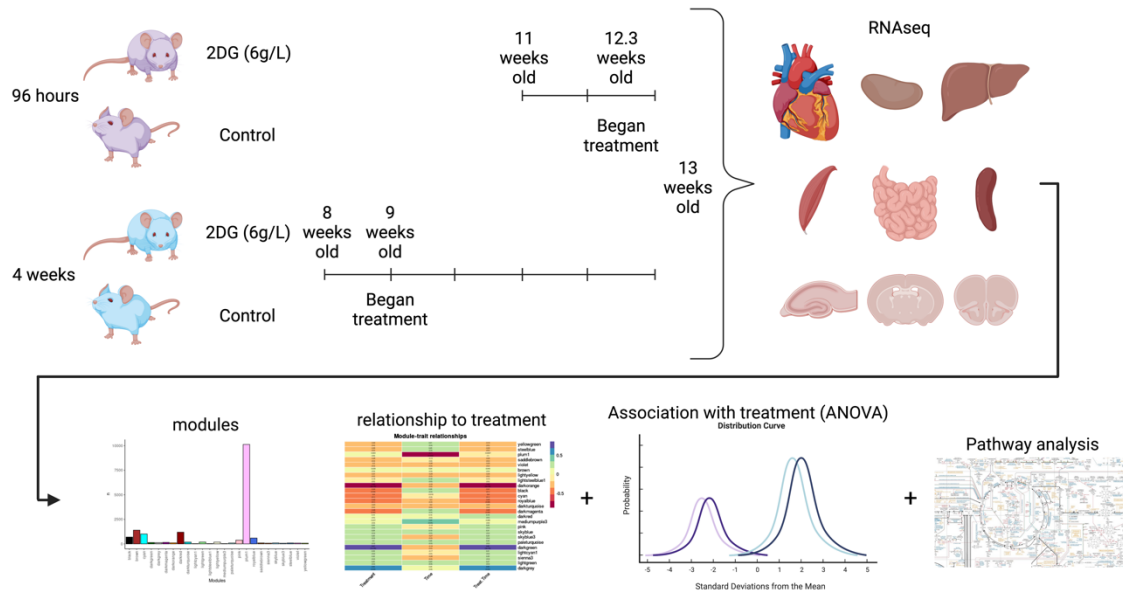
619 References

- 620 [1] Ben Sahra I, Tanti JF, Bost F. The combination of metformin and 2 deoxyglucose inhibits
621 autophagy and induces AMPK-dependent apoptosis in prostate cancer cells. *Autophagy*.
622 2010;6:670-1.
- 623 [2] Aft RL, Zhang FW, Gius D. Evaluation of 2-deoxy-D-glucose as a chemotherapeutic agent:
624 mechanism of cell death. *Br J Cancer*. 2002;87:805-12.
- 625 [3] Sottnik JL, Lori JC, Rose BJ, Thamm DH. Glycolysis inhibition by 2-deoxy-D-glucose reverts
626 the metastatic phenotype in vitro and in vivo. *Clin Exp Metastasis*. 2011;28:865-75.
- 627 [4] Cay O, Radnell M, Jeppsson B, Ahren B, Bengmark S. Inhibitory effect of 2-deoxy-D-glucose
628 on liver tumor growth in rats. *Cancer Res*. 1992;52:5794-6.
- 629 [5] Raez LE, Papadopoulos K, Ricart AD, Chiorean EG, Dipaola RS, Stein MN, et al. A phase I
630 dose-escalation trial of 2-deoxy-D-glucose alone or combined with docetaxel in patients with
631 advanced solid tumors. *Cancer Chemother Pharmacol*. 2013;71:523-30.
- 632 [6] Koenig JB, Cantu D, Low C, Sommer M, Noubary F, Croker D, et al. Glycolytic inhibitor 2-
633 deoxyglucose prevents cortical hyperexcitability after traumatic brain injury. *JCI Insight*. 2019;5.
- 634 [7] Sproule TJ, Wilson J, Adkins E, Crocker BP, Morel L, Roopenian DC. AI-19 Metabolic
635 inhibition by 2-deoxyglucose prevents and reverses lupus in mice. *Lupus Science &
636 Medicine*. 2016;3:A10-A.
- 637 [8] Wang H, Zhang N, Fang K, Chang X. 2-Deoxy-D-glucose Alleviates Collagen-Induced
638 Arthritis of Rats and Is Accompanied by Metabolic Regulation of the Spleen and Liver. *Front
639 Immunol*. 2021;12:713799.
- 640 [9] Aiestaran-Zelaia I, Sanchez-Guisado MJ, Villar-Fernandez M, Azkargorta M, Fadon-Padilla
641 L, Fernandez-Pelayo U, et al. 2 deoxy-D-glucose augments the mitochondrial respiratory chain
642 in heart. *Sci Rep*. 2022;12:6890.
- 643 [10] Bhatt AN, Shenoy S, Munjal S, Chinnadurai V, Agarwal A, Vinoth Kumar A, et al. 2-deoxy-
644 D-glucose as an adjunct to standard of care in the medical management of COVID-19: a proof-
645 of-concept and dose-ranging randomised phase II clinical trial. *BMC Infect Dis*. 2022;22:669.
- 646 [11] Pajak B, Zielinski R, Manning JT, Matejin S, Paessler S, Fokt I, et al. The Antiviral Effects of
647 2-Deoxy-D-glucose (2-DG), a Dual D-Glucose and D-Mannose Mimetic, against SARS-CoV-2
648 and Other Highly Pathogenic Viruses. *Molecules*. 2022;27.
- 649 [12] Sahu KK, Kumar R. Role of 2-Deoxy-D-Glucose (2-DG) in COVID-19 disease: A potential
650 game-changer. *J Family Med Prim Care*. 2021;10:3548-52.
- 651 [13] Pajak B, Siwiak E, Soltyka M, Priebe A, Zielinski R, Fokt I, et al. 2-Deoxy-d-Glucose and Its
652 Analogs: From Diagnostic to Therapeutic Agents. *Int J Mol Sci*. 2019;21.
- 653 [14] Xi H, Kurtoglu M, Liu H, Wangpaichitr M, You M, Liu X, et al. 2-Deoxy-D-glucose activates
654 autophagy via endoplasmic reticulum stress rather than ATP depletion. *Cancer Chemother
655 Pharmacol*. 2011;67:899-910.
- 656 [15] Zhao Q, Chu Z, Zhu L, Yang T, Wang P, Liu F, et al. 2-Deoxy-d-Glucose Treatment
657 Decreases Anti-inflammatory M2 Macrophage Polarization in Mice with Tumor and Allergic
658 Airway Inflammation. *Front Immunol*. 2017;8:637.
- 659 [16] Wang Q, Liang B, Shirwany NA, Zou MH. 2-Deoxy-D-glucose treatment of endothelial cells
660 induces autophagy by reactive oxygen species-mediated activation of the AMP-activated protein
661 kinase. *Plos One*. 2011;6:e17234.
- 662 [17] Yao J, Chen S, Mao Z, Cadenas E, Brinton RD. 2-Deoxy-D-glucose treatment induces
663 ketogenesis, sustains mitochondrial function, and reduces pathology in female mouse model of
664 Alzheimer's disease. *Plos One*. 2011;6:e21788.
- 665 [18] Abboud G, Choi SC, Kanda N, Zeumer-Spataro L, Roopenian DC, Morel L. Inhibition of
666 Glycolysis Reduces Disease Severity in an Autoimmune Model of Rheumatoid Arthritis. *Front
667 Immunol*. 2018;9:1973.

- 668 [19] Wang Y, Li JR, Sun MX, Ni B, Huan C, Huang L, et al. Triggering unfolded protein response
669 by 2-Deoxy-D-glucose inhibits porcine epidemic diarrhea virus propagation. *Antiviral Res.*
670 2014;106:33-41.
- 671 [20] Choi SC, Titov AA, Abboud G, Seay HR, Brusko TM, Roopenian DC, et al. Inhibition of
672 glucose metabolism selectively targets autoreactive follicular helper T cells. *Nat Commun.*
673 2018;9:4369.
- 674 [21] Langmead B, Salzberg SL. Fast gapped-read alignment with Bowtie 2. *Nat Methods.*
675 2012;9:357-9.
- 676 [22] McCarthy DJ, Chen Y, Smyth GK. Differential expression analysis of multifactor RNA-Seq
677 experiments with respect to biological variation. *Nucleic Acids Res.* 2012;40:4288-97.
- 678 [23] Robinson MD, McCarthy DJ, Smyth GK. edgeR: a Bioconductor package for differential
679 expression analysis of digital gene expression data. *Bioinformatics.* 2010;26:139-40.
- 680 [24] Chen Y, Lun AT, Smyth GK. From reads to genes to pathways: differential expression
681 analysis of RNA-Seq experiments using Rsubread and the edgeR quasi-likelihood pipeline.
682 *F1000Res.* 2016;5:1438.
- 683 [25] Team RC. R: A language and environment for statistical computing. Vienna, Austria: R
684 Foundation for Statistical Computing; 2022.
- 685 [26] Langfelder P, Horvath S. WGCNA: an R package for weighted correlation network analysis.
686 *BMC Bioinformatics.* 2008;9:559.
- 687 [27] Horvath PLS. Fast R Functions for Robust Correlations and Hierarchical Clustering. *Journal*
688 *of Statistical Software.* 2012;46:1-17.
- 689 [28] Raudvere LKU. gprofiler2: Interface to the 'g:Profiler' Toolset. R package version 0.2.0
690 ed2020.
- 691 [29] Kay ME, L; Higgins, J; Wobbrock, J. _ARTool: Aligned Rank Transform for Nonparametric
692 Factorial ANOVAs_. 2021.
- 693 [30] Wobbrock JF, L; Gergle, D; Higgins, J. The Aligned Rank Transform for Nonparametric
694 Factorial Analyses Using Only ANOVA Procedures. *Proceedings of the ACM*
695 *Conference on Human Factors in Computing Systems (CHI '11).* 2011:143-6.
- 696 [31] Imai DTTYKHLKK. mediation: R Package for Causal Mediation Analysis. *Journal of*
697 *Statistical Software.* 2014;59:1-38.
- 698 [32] Hänzelmann SC, R.; Guinney, A. GSEA: gene set variation analysis for microarray and
699 RNA-seq data. *BMC Bioinformatics.* 2013;14.
- 700 [33] Xie Y. bookdown: authoring Books and Technical Documents with R markdown: Chapman
701 and Hall/CRC; 2016.
- 702 [34] Ye Z, Wang S, Zhang C, Zhao Y. Coordinated Modulation of Energy Metabolism and
703 Inflammation by Branched-Chain Amino Acids and Fatty Acids. *Front Endocrinol (Lausanne).*
704 2020;11:617.
- 705 [35] Jiang M, Xie X, Cao F, Wang Y. Mitochondrial Metabolism in Myocardial Remodeling and
706 Mechanical Unloading: Implications for Ischemic Heart Disease. *Front Cardiovasc Med.*
707 2021;8:789267.
- 708 [36] Adeva-Andany MM, Gonzalez-Lucan M, Donapetry-Garcia C, Fernandez-Fernandez C,
709 Ameneiros-Rodriguez E. Glycogen metabolism in humans. *BBA Clin.* 2016;5:85-100.
- 710 [37] Xie N, Zhang L, Gao W, Huang C, Huber PE, Zhou X, et al. NAD(+) metabolism:
711 pathophysiologic mechanisms and therapeutic potential. *Signal Transduct Target Ther.*
712 2020;5:227.
- 713 [38] Liu L, Su X, Quinn WJ, 3rd, Hui S, Krukenberg K, Frederick DW, et al. Quantitative Analysis
714 of NAD Synthesis-Breakdown Fluxes. *Cell Metab.* 2018;27:1067-80 e5.
- 715 [39] Aebi M. N-linked protein glycosylation in the ER. *Biochim Biophys Acta.* 2013;1833:2430-7.
- 716 [40] Hue L, Taegtmeyer H. The Randle cycle revisited: a new head for an old hat. *Am J Physiol*
717 *Endocrinol Metab.* 2009;297:E578-91.

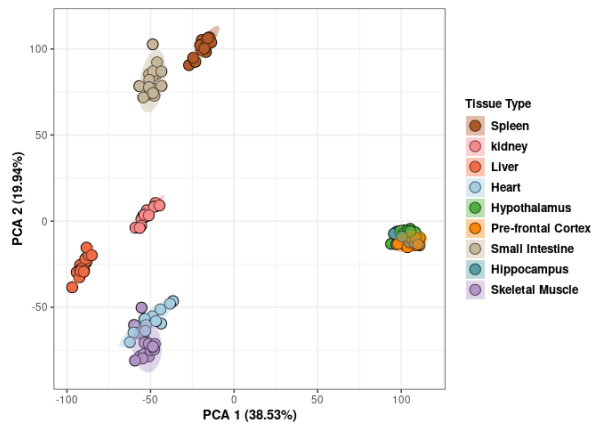
- 718 [41] Moncan M, Mnich K, Blomme A, Almanza A, Samali A, Gorman AM. Regulation of lipid
719 metabolism by the unfolded protein response. *J Cell Mol Med.* 2021;25:1359-70.
- 720 [42] Calder PC. Branched-chain amino acids and immunity. *J Nutr.* 2006;136:288S-93S.
- 721 [43] Baakhtari M, Imaizumi N, Kida T, Yanagita T, Ramah A, Ahmadi P, et al. Effects of
722 branched-chain amino acids on immune status of young racing horses. *J Vet Med Sci.*
723 2022;84:558-65.
- 724 [44] Yahsi B, Gunaydin G. Immunometabolism - The Role of Branched-Chain Amino Acids.
725 *Front Immunol.* 2022;13:886822.
- 726 [45] Mu WC, VanHoosier E, Elks CM, Grant RW. Long-Term Effects of Dietary Protein and
727 Branched-Chain Amino Acids on Metabolism and Inflammation in Mice. *Nutrients.* 2018;10.
- 728 [46] Lee D, Hokinson D, Park S, Elvira R, Kusuma F, Lee JM, et al. ER Stress Induces Cell
729 Cycle Arrest at the G2/M Phase Through eIF2alpha Phosphorylation and GADD45alpha. *Int J*
730 *Mol Sci.* 2019;20.
- 731 [47] Dwarakanath B, Jain V. Targeting glucose metabolism with 2-deoxy-D-glucose for
732 improving cancer therapy. *Future Oncol.* 2009;5:581-5.
- 733 [48] Ciavardelli D, Rossi C, Barcaroli D, Volpe S, Consalvo A, Zucchelli M, et al. Breast cancer
734 stem cells rely on fermentative glycolysis and are sensitive to 2-deoxyglucose treatment. *Cell*
735 *Death Dis.* 2014;5:e1336.
- 736 [49] Chiaravalli M, Rowe I, Mannella V, Quilici G, Canu T, Bianchi V, et al. 2-Deoxy-d-Glucose
737 Ameliorates PKD Progression. *J Am Soc Nephrol.* 2016;27:1958-69.
- 738 [50] Tailler M, Lindqvist LM, Gibson L, Adams JM. By reducing global mRNA translation in
739 several ways, 2-deoxyglucose lowers MCL-1 protein and sensitizes hemopoietic tumor cells to
740 BH3 mimetic ABT737. *Cell Death Differ.* 2019;26:1766-81.
- 741 [51] Sun H, Olson KC, Gao C, Prosdocimo DA, Zhou M, Wang Z, et al. Catabolic Defect of
742 Branched-Chain Amino Acids Promotes Heart Failure. *Circulation.* 2016;133:2038-49.
- 743 [52] Neinast MD, Jang C, Hui S, Murashige DS, Chu Q, Morscher RJ, et al. Quantitative
744 Analysis of the Whole-Body Metabolic Fate of Branched-Chain Amino Acids. *Cell Metab.*
745 2019;29:417-29 e4.
- 746 [53] Stein M, Lin H, Jeyamohan C, Dvorzhinski D, Gounder M, Bray K, et al. Targeting tumor
747 metabolism with 2-deoxyglucose in patients with castrate-resistant prostate cancer and
748 advanced malignancies. *Prostate.* 2010;70:1388-94.
- 749 [54] Wiertsema SP, van Bergenhenegouwen J, Garssen J, Knippels LMJ. The Interplay
750 between the Gut Microbiome and the Immune System in the Context of Infectious Diseases
751 throughout Life and the Role of Nutrition in Optimizing Treatment Strategies. *Nutrients.* 2021;13.
- 752 [55] Cai W, Cheng J, Zong S, Yu Y, Wang Y, Song Y, et al. The glycolysis inhibitor 2-
753 deoxyglucose ameliorates adjuvant-induced arthritis by regulating macrophage polarization in
754 an AMPK-dependent manner. *Mol Immunol.* 2021;140:186-95.
- 755 [56] Houten SM, Violante S, Ventura FV, Wanders RJ. The Biochemistry and Physiology of
756 Mitochondrial Fatty Acid beta-Oxidation and Its Genetic Disorders. *Annu Rev Physiol.*
757 2016;78:23-44.
- 758 [57] McFadden JW, Aja S, Li Q, Bandaru VV, Kim EK, Haughey NJ, et al. Increasing fatty acid
759 oxidation remodels the hypothalamic neurometabolome to mitigate stress and inflammation.
760 *Plos One.* 2014;9:e115642.
- 761 [58] Butterfield DA, Favia M, Spera I, Campanella A, Lanza M, Castegna A. Metabolic Features
762 of Brain Function with Relevance to Clinical Features of Alzheimer and Parkinson Diseases.
763 *Molecules.* 2022;27.
- 764 [59] Trinh MA, Kaphzan H, Wek RC, Pierre P, Cavener DR, Klann E. Brain-specific disruption of
765 the eIF2alpha kinase PERK decreases ATF4 expression and impairs behavioral flexibility. *Cell*
766 *Rep.* 2012;1:676-88.

- 767 [60] Kim P, Scott MR, Meador-Woodruff JH. Dysregulation of the unfolded protein response
768 (UPR) in the dorsolateral prefrontal cortex in elderly patients with schizophrenia. *Mol Psychiatry*.
769 2021;26:1321-31.
- 770 [61] Ajoolahady A, Lindholm D, Ren J, Pratico D. ER stress and UPR in Alzheimer's disease:
771 mechanisms, pathogenesis, treatments. *Cell Death Dis*. 2022;13:706.
- 772 [62] Shi H, Scheffler JM, Zeng C, Pleitner JM, Hannon KM, Grant AL, et al. Mitogen-activated
773 protein kinase signaling is necessary for the maintenance of skeletal muscle mass. *Am J*
774 *Physiol Cell Physiol*. 2009;296:C1040-8.
- 775 [63] Penna F, Costamagna D, Fanzani A, Bonelli G, Baccino FM, Costelli P. Muscle wasting
776 and impaired myogenesis in tumor bearing mice are prevented by ERK inhibition. *Plos One*.
777 2010;5:e13604.
- 778 [64] Seaberg B, Henslee G, Wang S, Paez-Colasante X, Landreth GE, Rimer M. Muscle-
779 derived extracellular signal-regulated kinases 1 and 2 are required for the maintenance of adult
780 myofibers and their neuromuscular junctions. *Mol Cell Biol*. 2015;35:1238-53.
- 781 [65] Francis R, Singh PK, Singh S, Giri S, Kumar A. Glycolytic inhibitor 2-deoxyglucose
782 suppresses inflammatory response in innate immune cells and experimental staphylococcal
783 endophthalmitis. *Exp Eye Res*. 2020;197:108079.
- 784 [66] Wen X, Zhang B, Wu B, Xiao H, Li Z, Li R, et al. Signaling pathways in obesity:
785 mechanisms and therapeutic interventions. *Signal Transduct Target Ther*. 2022;7:298.
786

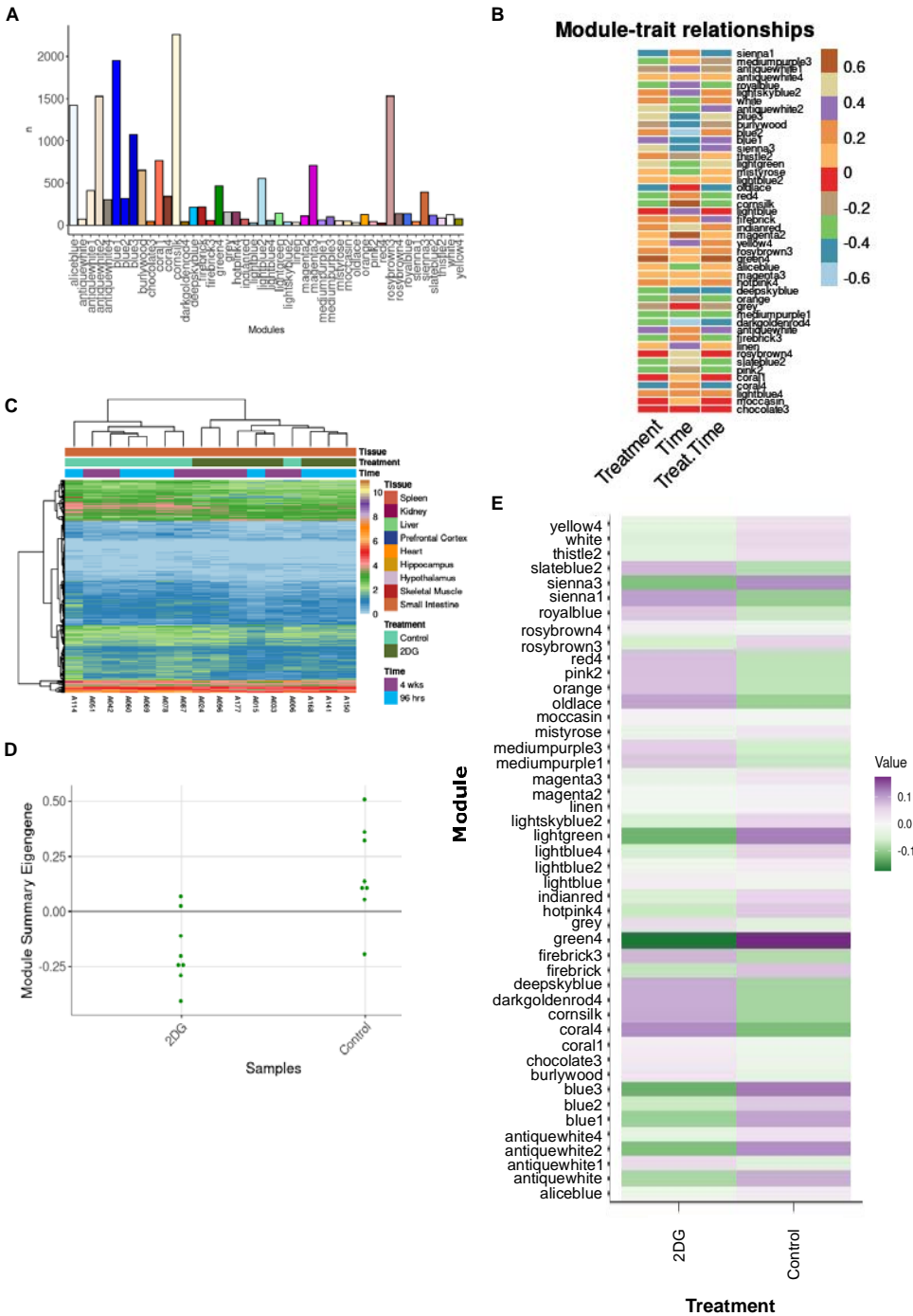


Created with Biorender.com

787
 788 **Figure 1:** Experimental Design and analysis flow. C57BL/6J mice were treated with 2DG (6g/L)
 789 for 96 hours or 4 weeks. Nine tissues were harvested for bulk transcriptomics. Genes identified
 790 for each tissue were clustered into modules using WGCNA. Effects of 2DG on each module
 791 were determined by assessing each modules relationship with treatment through correlation,
 792 ANOVA, and pathway analysis. Created with Biorender.com
 793

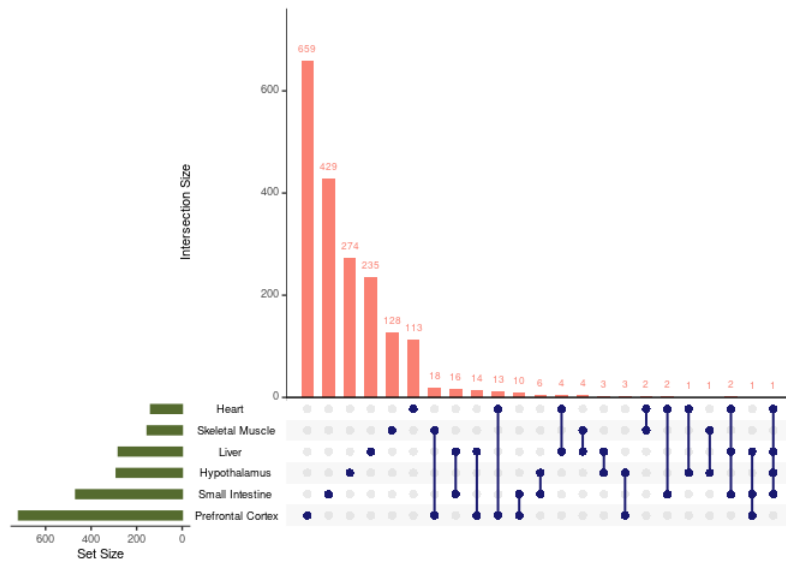


794
 795 **Figure 2:** Principal Component Analysis demonstrated clustering of samples based on tissue
 796 type. Hotelling's T^2 ellipses were calculated, and the clustering patterns of all tissue were
 797 contained within the 95% confidence intervals.
 798



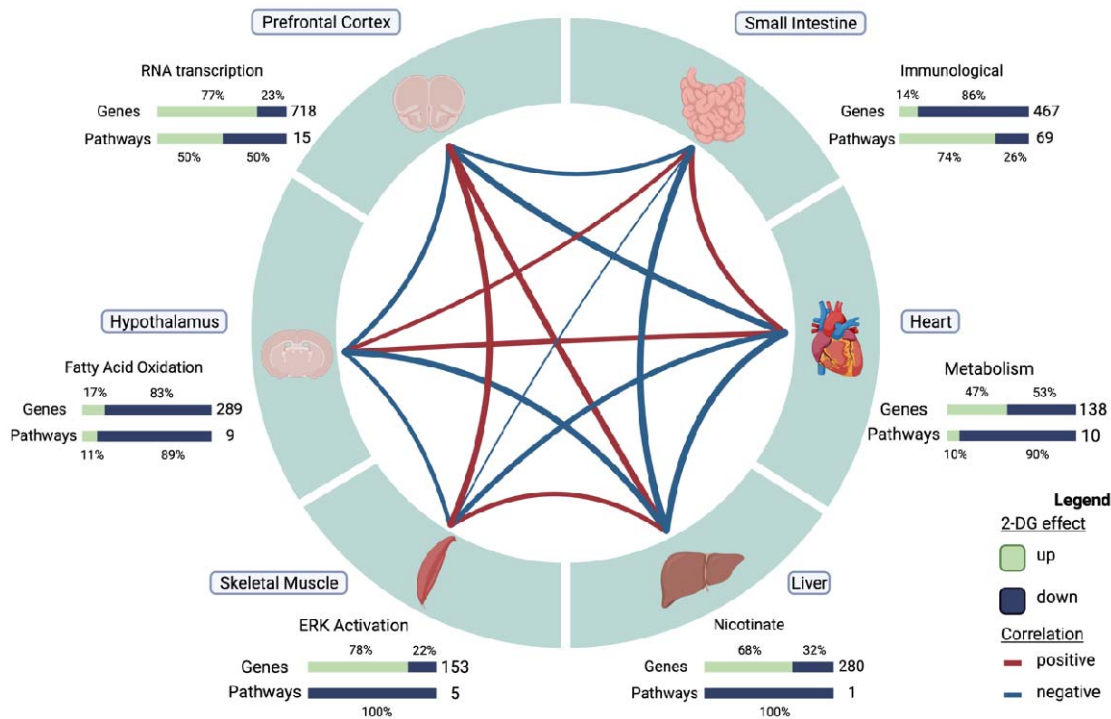
799
 800 **Figure 3:** Analysis of modules-treatment association. A) A total of 46 modules were identified in
 801 the small intestine, each containing between 22 and 2,259 genes. B) Correlation analysis
 802 between time, treatment, and treatment in a time dependent manner revealed three modules
 803 significantly correlated with treatment. C) The average eigengene expression of the green4
 804 module shows that expression levels are lower in mice treated with 2DG compared to control
 805 mice. D) Summary eigengene expression for each sample in the green4 module confirms lower
 806 expression in mice treated with 2DG compared to control mice., and E) Individual genes across
 807 samples clustered by treatment except for one control sample, which clustered with 2DG-
 808 treated mice.

809



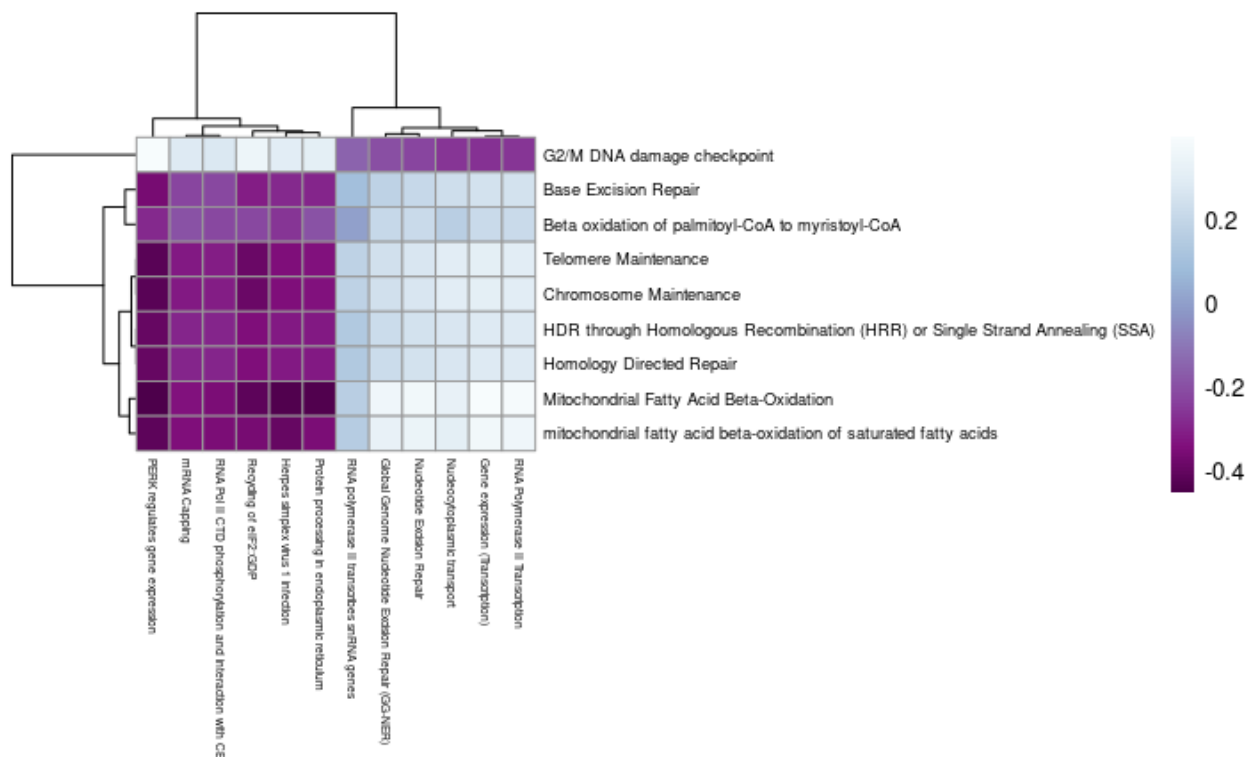
810
811
812
813
814

Figure 4: Number of identified genes shared between tissue modules. Each dot represents the tissue or tissues being compared. Very few genes were shared across tissues and no gene was shared across all tissues. Only tissue combinations with one or more shared genes are shown.



815
816
817
818
819
820
821

Figure 5: Correlation structure of gene module changes across tissues in 2-DG-treated mice. Six tissues, each represented by one high confidence module, demonstrated unique response to 2-DG treatment. The expression levels of genes and pathways within each tissue showed varying degrees of over- and under-expression in response to 2-DG. Created with Biorender.com.



830
 831 **Figure 7:** Correlations between pathway eigengenes in the hypothalamus (y-axis) and
 832 prefrontal cortex (x-axis). G2/M DNA damage checkpoint in the hypothalamus was negatively
 833 correlated with pathways related to ER stress and positively correlated with pathways related to
 834 RNA transcription in the prefrontal cortex. All other metabolic pathways in the hypothalamus
 835 were positively correlated with pathways related to ER stress and negatively correlated with
 836 pathways related to RNA transcription in the prefrontal cortex.